frontiers in Materials

ORIGINAL RESEARCH
published: 10 December 2019
doi: 10.3389/fmats.2019.00321

Microstructural Characteristics and Mechanical Properties of a Novel Extruded Dilute Mg–Sn–Mn–Ca Alloy

Ming-ya Zhang[1], *Mei-juan Hao*[2], *Wei-li Cheng*[2,3]*, *Jinghui Li*[1], *Chen Guo*[2], *Xiao-feng Niu*[2,3], *Hong-xia Wang*[2] *and Li-fei Wang*[2]

[1] School of Metallurgical Engineering, Anhui University of Technology, Ma'anshan, China, [2] School of Materials Science and Engineering, Taiyuan University of Technology, Taiyuan, China, [3] Shanxi Key Laboratory of Advanced Magnesium-Based Materials, Taiyuan University of Technology, Taiyuan, China

A novel dilute Mg-Sn-Mn-Ca (TMX) alloy system was developed and subjected to extrusion with a relatively high extrusion ratio of 36. The grain structure, nanoscale precipitates, texture, and tensile properties of the extruded dilute alloy were investigated. The results indicated that complete dynamic recrystallization (DRX) together with some nanoscale and/or sub-microscale Mg_2Sn and Mg_2Ca precipitates could be obtained after extrusion. The tensile yield strength, ultimate tensile strength and elongation of the extruded dilute alloy were 213 and 266 MPa, and 21%, respectively. The correlation between microstructural characteristics and properties was also discussed.

Keywords: Mg-Sn-based alloy, dynamic recrystallization, extrusion, texture, tensile properties

OPEN ACCESS

Edited by:
Seunghwa Ryu,
Korea Advanced Institute of Science & Technology (KAIST), South Korea

Reviewed by:
Dongchan Jang,
Korea Advanced Institute of Science & Technology (KAIST), South Korea
Changguo Wang,
Harbin Institute of Technology, China

***Correspondence:**
Wei-li Cheng
chengweili7@126.com

Specialty section:
This article was submitted to Mechanics of Materials, a section of the journal Frontiers in Materials

Received: *27 July 2019*
Accepted: *22 November 2019*
Published: *10 December 2019*

Citation:
Zhang M, Hao M, Cheng W, Li J, Guo C, Niu X, Wang H and Wang L (2019) Microstructural Characteristics and Mechanical Properties of a Novel Extruded Dilute Mg–Sn–Mn–Ca Alloy. Front. Mater. 6:321. doi: 10.3389/fmats.2019.00321

INTRODUCTION

It is generally accepted that Mg-Sn-based alloys have better strength and ductility than commercial Mg-Al-based alloys after extrusion under identical conditions (Park et al., 2016; She et al., 2016; Cheng et al., 2017b; Lu et al., 2018b). Recently, a system of Mg-Sn-based alloys with high Sn content, containing thermally stable Mg_2Sn phase has exhibited an excellent extrudability (Sasaki et al., 2008; Cheng et al., 2010). However, a high Sn content would cause a significant increase in the cost of the final products. Moreover, the extruded Mg-Sn-based alloys with high Sn content commonly have sub-microscale and microscale Mg_2Sn particles co-existing at the grain boundary in the form of network, which prevents further performance improvement (Cheng et al., 2010). Many previous reports have verified that decreasing the alloying element contents of Mg alloys could efficiently reduce the thermally stable phase contents and modify the morphologies of the strengthening precipitates (Hofstetter et al., 2015; Pan et al., 2018; Wang et al., 2018; Hu et al., 2019), thus improving the extrudability and ductility. Accordingly, studies have recently been concentrated on micro-alloyed systems with low content of Sn in order to reduce the cost of products (Chai et al., 2019a). She et al. (2016) proposed that the addition of 1 wt.% Sn content in Mg alloys is expected to exhibit a great balance between strength and ductility.

With the aim of promoting further application of Mg-1Sn alloy system, micro-alloying by adding other elements is required. In recent years, Ca element has attracted increasing attention because of their low cost and universal existence. The addition of low content of Ca was reported to modify the extrusion texture, leading to improved ductility in dilute Mg-1.0Zn-0.5Ca alloy (Zhang et al., 2012). Furthermore, relevant studies (Wei et al., 2013; Lu et al., 2018a) have shown that the grain size and grain boundary compound of such alloys could be refined significantly via the trace addition of Ca, thus improving the formability. Besides, Mn is an appropriate alloy element to

improve the mechanical properties and to optimize the microstructure of Mg alloys (Liao et al., 2019). It was reported that the growth of DRX grains during hot extrusion could be inhibited by the addition of low Mn content, and thus excellent tensile properties was obtained (Tong et al., 2011; Chen et al., 2016; Lu et al., 2018a). Liao et al. (2019) fabricated a system of Mg-1Sn-Mn based alloys with high mechanical properties through extrusion. Chai et al. (2019b) reported that Mg-1Sn-0.5Zn based alloys exhibited improved tensile ductility via the addition of low amount of Ca ($\leq$1 wt.%). While, there have been rarely few reports on the combined addition of low content of Mn and Ca to the Mg-1Sn based alloys thus far.

Besides alloying, extrusion is one of the most effective plastic deformation methods to improve the ductility and stretch formability of Mg-based alloys via refining grain structure (Lu et al., 2018b). It was also reported that increasing the extrusion ratio contributes to the formation of uniform structure with complete DRX (Yu et al., 2019). Therefore, a novel dilute Mg-1.0Sn-0.5Mn-0.5Ca alloy system with a good balance between extrudability and ductility was developed and subjected to extrusion with a relatively high extrusion ratio of 36. The grain structure, orientations, nanoscale precipitates, and resultant mechanical properties of the dilute extruded alloy were discussed in detail.

EXPERIMENTAL PROCEDURE

The ingot with a nominal composition of Mg-1.0Sn-0.5Mn-0.5Ca (wt.%) (TMX-1.0) was prepared by melting commercially pure Mg (99.9 wt.%), Sn (99.99 wt.%), Mg-30%Ca and Mg-10%Mn master alloys in an electrical resistance furnace under a ($SF_6 + CO_2$) fluxing protection to avoid oxidation. After casting, solution treatment of the as-cast ingot with a diameter and length of 75 and 65 mm, respectively, was conducted at 320°C for 3 h and then 500°C for 1 h, followed by water-quenching. After preheating at 300°C for 30 min, the alloy ingot was extruded at 300 °C with a ram speed of 0.1 mm/s and an extrusion ratio of 36.

The as-extruded specimen was sectioned parallel to the extrusion direction (ED) for microstructural examinations. The average size of grains was measured using Image-Pro Plus 6.0 software based on five optical microscopic (OM; Leica 2700 M) micrographs after a conventional metallographic procedure (including grinding, polishing, and etching in a solution of 1.5 g picric acid, 5 ml acetic acid, 5 ml H_2O, and 25 ml ethanol). The morphologies of precipitates were observed using transmission electron microscopy (TEM; JEM-2100F operated at 200 kV). Thin foil samples for the TEM observations were prepared by ion milling using a Precision Ion Polishing System. Phase identification was performed by X-ray diffraction (XRD; Cu-Kα, Y-2000) and selected-area diffraction patterns (SADP). The microscopic texture of the as-extruded sample was measured at a step size of 1.4 μm using a field-emission scanning electron microscope (Carl Zeiss CrossBeam 1540EsB) equipped with an electron backscatter diffraction (EBSD) detector operating at 20 Kv and HKL Channel 5 acquisition software. Microhardness tests were performed using a microhardness tester with indentation loads from 0.490 to 4.903 N for 15 s. Tensile specimens (dog-bone-shaped) with a gauge dimension of 18 mm in length, 4 mm in width and 2 mm in thickness were prepared from the extruded rod along the ED. Tensile tests were then performed at room temperature using a DNS100 electric testing machine with an initial strain rate of 1×10^{-3} s^{-1}. Tensile tests were performed three times to obtain the average values reported in this work.

RESULTS AND DISCUSSION

Microstructural Characteristics

Grain Structure

The microstructure of the extruded TMX-1.0 alloy is shown in **Figure 1**. The studied alloy exhibits fully recrystallized structure after extrusion. The distribution of grain size is uniform and the average grain size is 12.25 ± 0.15 μm. In addition, some low angle grain boundaries indicated by laurel-green line could also be observed, which indicated that the dynamic recrystallization (DRX) mechanism for the studied alloy is continuous DRX dominated. Furthermore, the presence of nano-scaled precipitates and solutioned Sn in the matrix are beneficial to refine the size of DRX grains through Zener-drag effect (Robson et al., 2009; Fang et al., 2017; Zhao et al., 2018).

Dynamic Precipitates

Figure 2 illustrates the XRD results of the extruded dilute TMX-1.0 alloy. The results indicate that the studied alloy mainly comprises α-Mg, Mg_2Sn, and Mg_2Ca phases. It was reported that Mg_2Ca rather than CaMgSn phase was formed in Mg-Sn-Ca-based alloys when the Sn/Ca mass ratios were lower than ∼2.5:1 (Chai et al., 2019a). The intensities of the peaks corresponding to the Mg_2Sn and Mg_2Ca phases in the extruded dilute alloy are relatively weak because of the low concentrations of alloying elements.

The TEM images of the studied alloy are shown in **Figure 3**. Some fine nanoscale and sub-microscale precipitates can be observed in certain micro-domains. Many previous studies have reported the formation of nanoscale precipitates through dynamic precipitation in the extruded Mg alloys (Fang et al., 2017). Analyses of the SADP results indicate that the precipitates are Mg_2Ca, which has a hexagonal structure, and Mg_2Sn, respectively. The Mg_2Sn borders on Mg_2Ca, indicating that the Mg_2Ca phase is the nucleation site of Mg_2Sn. The formation of Mg_2Ca consumes Ca, providing Sn-enriched regions between the Mg_2Ca phase and matrix herein. A similar phenomenon was found in previous report (Xu and Han, 2012).

Texture Evolution

The EBSD results of the studied alloy are presented in **Figure 4**. Most of the grains are tilted by ∼30° from the center of the (0002) pole figure to the ED with the texture intensity being 9.23 (**Figure 4b**). The relatively strong basal texture may be ascribed to the addition of Mn (Liao et al., 2019). Additionally, the correlations between grain size and texture of the extruded dilute alloy are shown in **Figure 4c**, in which the total grains are classified into two categories using the grain size of 12 μm as a benchmark. It turns out that these two halves of the grains

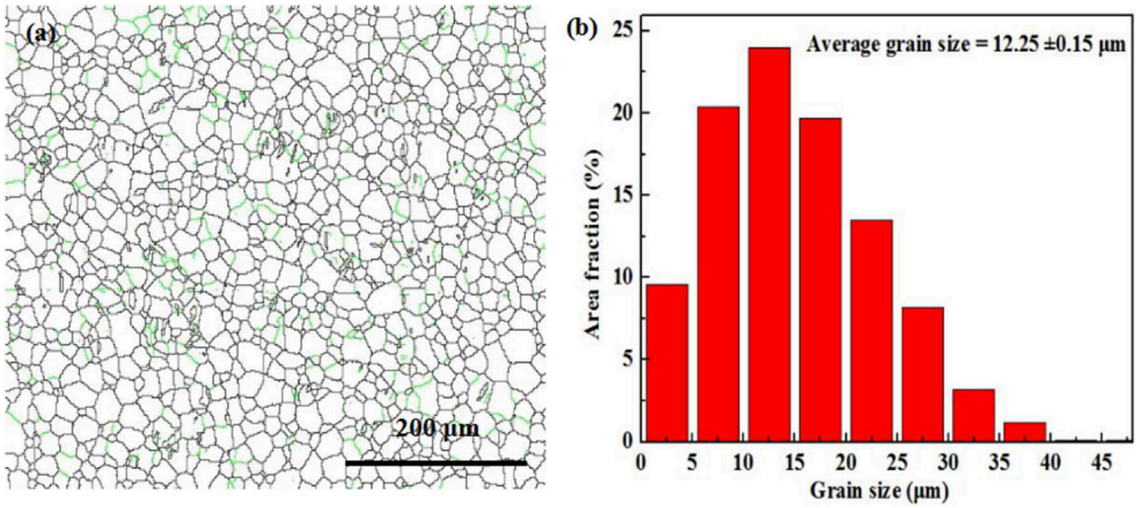

FIGURE 1 | (a) Grain boundary orientation image and **(b)** grain size distribution of extruded dilute TMX-1.0 alloy. Low angle GBs were highlighted in laurel-green in **(a)**.

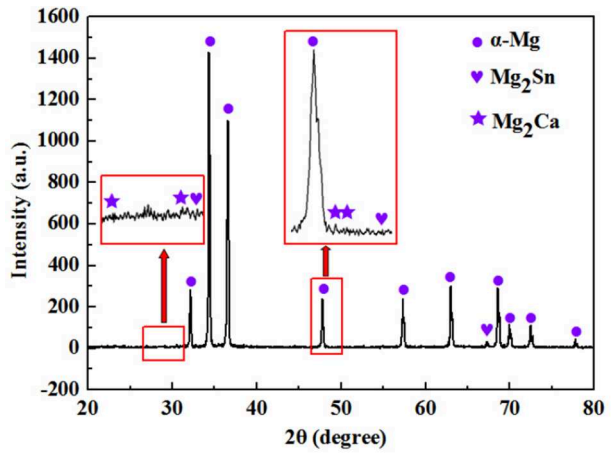

FIGURE 2 | The XRD pattern of the extruded dilute TMX-1.0 alloy.

each reveal the ED-titled basal texture, but the maximum texture intensity varies. It can be concluded that the texture intensity of the grains of >12 μm is much stronger than that of the smaller ones, indicating that the textural strengthening in the extruded dilute TMX-1.0 alloy is associated with the higher fraction (89.7%) of the relatively coarse grains (> 12 μm), which exhibit strong texture. Similar results could be also found in Cheng et al. (2010).

Indentation Size Effect

As an economical and effective method to evaluate the nanoscale mechanical behavior of materials, indentation test has been widely used. Moreover, previous report validated that strain-hardening behavior is closely related to the indentation size effect (ISE) (Yang, 2000). In order to study the indentation size effect (ISE), which shows an increase in hardness with decreasing applied load, different indentation loads ranging from 0.490 to 4.903 N are applied to the extruded dilute TMX-1.0 alloy and the related results are shown in **Figure 5A**. The microhardness values of TMX-1.0 alloy decreased from 47.7 to 40.8 HV with increasing the loads. Based on Meyer's expression, the load P and the indentation size d of the TMX-1.0 alloy can be calculated by the equation (Yang, 2000; Manika and Maniks, 2006; Valdez et al., 2012):

$$P = kd^n \tag{1}$$

where k and n are the Meyer prefactor and Meyer exponent, respectively. The corresponding n value could be obtained from Equation (1). By taking the natural logarithms of both sides of Equations (1) and (2) could be obtained:

$$\ln P = n \ln d + \ln k \tag{2}$$

Using Equation (2), linear fitting between ln P and ln d could be applied and the slope of the resulting line, namely the n value, could be deduced from the fitting results (**Figure 5B**). The ISE behavior can be assessed using the n value: in general, $n < 2$ implies that the microhardness is load-dependent in a material. The value of n in the extruded dilute alloy is 1.83 ± 0.063, indicating an ISE phenomenon. As shown in **Figure 5A**, the microhardness of the studied alloy decreases continuously with the increase of applied load, which may be due to the fact that basal slip systems can be activated easily under small strain, but blocked with increasing the strain within the load applied in this study (Yang, 2000).

Tensile Properties

The engineering tensile stress-strain curve and the corresponding work-hardening response of the extruded dilute TMX-1.0 alloy are shown in **Figure 6**. The tensile yield strength, ultimate tensile strength and elongation of the extruded dilute alloy are 213 and

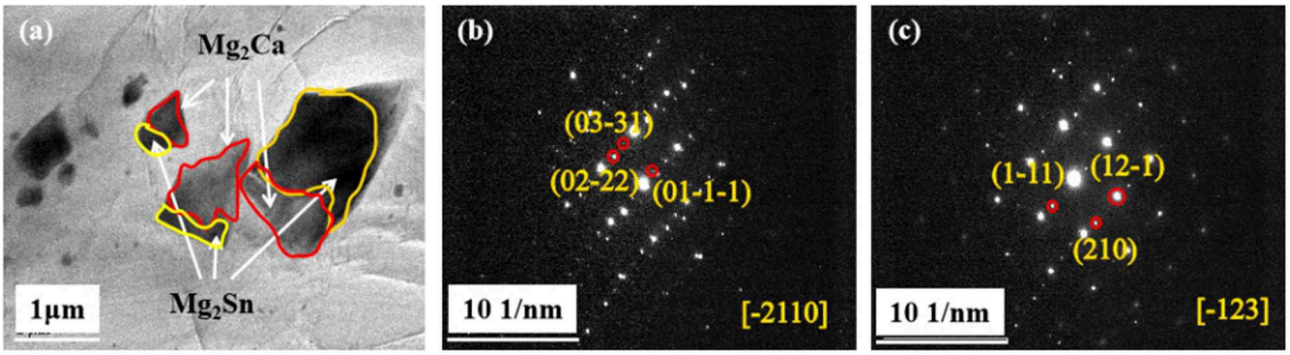

FIGURE 3 | (a) Bright field TEM image of the extruded dilute TMX-1.0 alloy; **(b)** Selected area electron diffraction (SAED) of Mg_2Ca; and **(c)** SAED of Mg_2Sn.

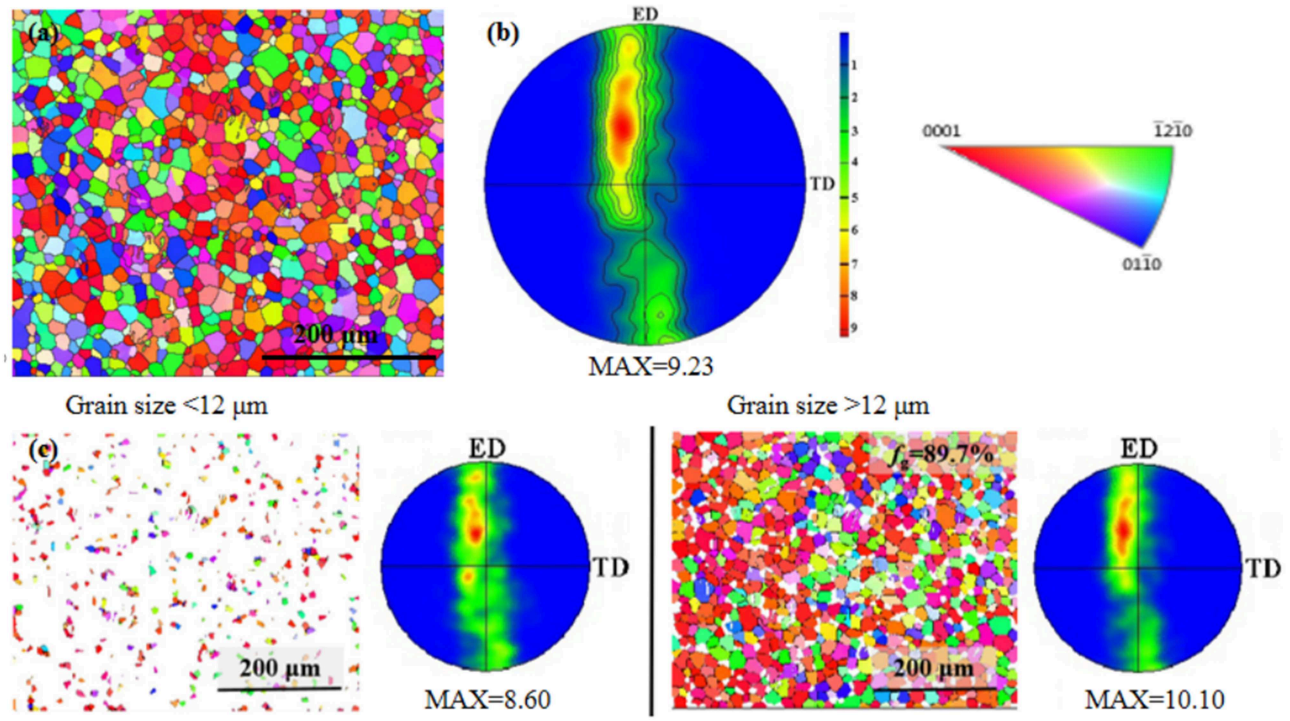

FIGURE 4 | EBSD results of the extruded TMX-1.0 alloy. **(a)** Inverse pole figure (IPF) map; **(b)** (0002) pole figure with respect to the extrusion direction (ED) and transverse direction (TD); **(c)** IPF maps and (0002) pole figures corresponding to grains with sizes <12 μm and >12 μm, respectively.

266 MPa, and 21%, respectively. **Figure 7** gives the comparison of tensile properties among the extruded dilute TMX-1.0 alloy in the present study with other Mg-based extruded alloys. It should be noted that TYS of the studied alloy is higher than that of Mg-Al and/or Mg-Zn based alloys studied in Refs. Tang et al. (2011), Nakata et al. (2015), Kim and Park (2016), Bae et al. (2018), Xiao et al. (2019), and Chai et al. (2019b). Some reported Mg-Al-Zn alloys exhibit higher TYS (Park et al., 2015; Kim et al., 2017), while these alloys present relatively poor elongation when compared with the studied TMX-1.0 alloy. Overall, the combined tensile properties of the studied alloy are at an acceptable level.

Figure 6B represents the work-hardening rate curve based on $\theta = \frac{d\sigma}{d\varepsilon}$, where σ and ε are the true stress and strain, respectively, for the extruded dilute TMX-1.0 alloy. By taking the natural logarithms of both sides of the Hollomon equation, the work-hardening exponent can be obtained. The calculated result is 0.13 for the studied alloy. Generally, a higher work-hardening exponent corresponds to lower sensitivity to strain localization, i.e., a greater EL (Tang et al., 2011; Zhao et al., 2018).

In general, the TYS of wrought Mg alloys is associated with grain size and orientation, as well as precipitates. The relationship between the grain size (d) and the yield

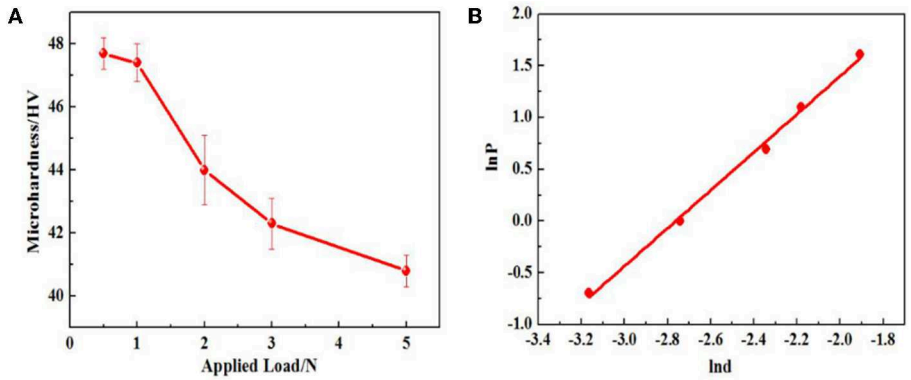

FIGURE 5 | Variations of micro-hardness with applied load for extruded dilute TMX-1.0 alloy **(A)** and the linear fit of lnP **(B)**.

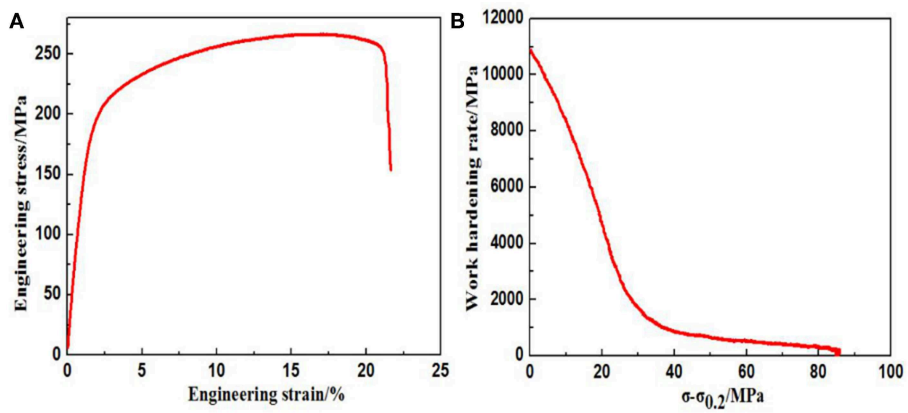

FIGURE 6 | The tensile properties of the extruded dilute TMX-1.0 alloy: **(A)** typical ambient-temperature tensile stress-strain curve, and **(B)** the working hardening response.

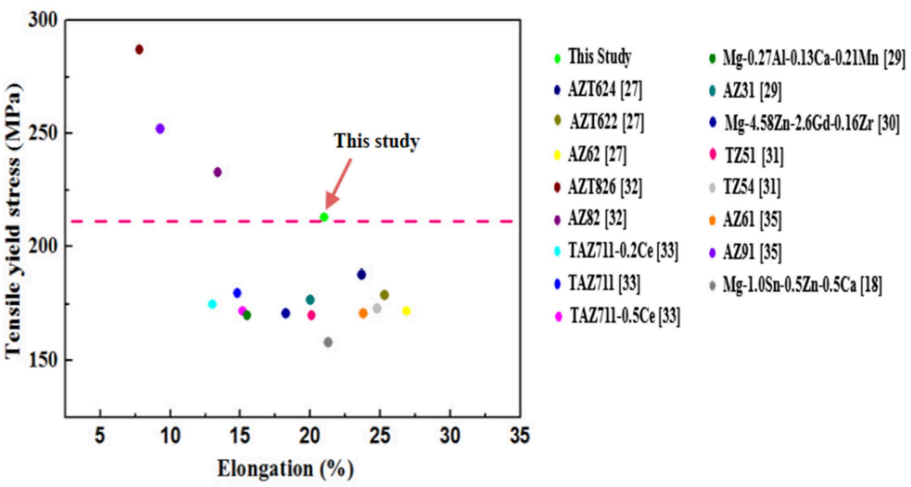

FIGURE 7 | The comparison of tensile properties among the extruded dilute TMX-1.0 alloy with other Mg-based extruded alloys.

TABLE 1 | Summary of average grain size (d_{avg}), basal texture intensity and tensile properties in different Mg alloy systems in literature and this study.

Alloy [Reference]	Basal texture intensity	d_{avg} (μm)	TYS (MPa)	UTS (MPa)	EL (%)
TMX-1.0 [this study]	9.23	12.25	213	266	21
Mg-1.0Sn-0.5Zn-0.5Ca (Chai et al., 2019b)	7.59	5.8	158.7	302	21.3
AZT624 (Bae et al., 2018)	2.9	5.3	188	330	23.7
AZT622 (Bae et al., 2018)	2.8	7.9	179	320	25.3
AZ62 (Bae et al., 2018)	3.2	8.3	172	313	26.9
AZ31 (Nakata et al., 2015)	–	48	177	–	20
Mg-0.27Al-0.13Ca-0.21Mn (Nakata et al., 2015)	–	27	170	–	15.5
TZ51 (Tang et al., 2011)	2.5	7.4	170	250	20.1
TZ54 (Tang et al., 2011)	2.8	6.9	173	287	24.8
AZT826 (Park et al., 2015)	1.9	1.2	287	354	7.8
AZ82 (Park et al., 2015)	2.4	2.2	233	347	13.4

strength is described using the Hall–Petch equation as follows (Cheng et al., 2014, 2017a,c):

$$\sigma_{gb} = \sigma_0 + Kd^{-1/2} \tag{3}$$

where σ_{gb} represents the contribution of grain boundary strengthening to the TYS, σ_0 is the material constant (21 MPa), and K is the Hall–Petch slope (280 MPa $\mu m^{-1/2}$). The calculated result shows that the increment in YS by reason of grain boundary is ∼101 MPa. From this respect, it is easily deduced that the improvement of TYS of the extruded dilute TMX-1.0 alloy is greatly dominated by grain boundary strengthening.

The effect of texture on the strength for Mg-Sn based alloys could be expressed as:

$$\sigma_{tex} = m\tau_0 \tag{4}$$

where m and τ_0 are orientation factor related to the (0002) basal texture, and critical resolved shear stress for basal slip system. In this study, m and τ_0 can be evaluated as 60 and 0.66, respectively (detailed information is presented in Cheng et al., 2018). Consequently, the relative contributions from texture strengthening is ∼39.6 MPa. Therefore, relativity high texture intensity of 9.23 for the studied alloy is advantageous to the improvement of tensile strength in a certain degree.

Many previous studies have reported that the nanoscale particles dynamically precipitated during extrusion can obstruct dislocation slip based on the Orowan mechanism (Stanford and Barnett, 2008; Tang et al., 2011; Cheng et al., 2014; Qi et al., 2014; Wang et al., 2016). However, the total fraction of the precipitates in the studied alloy is relatively low, and it was not clear whether this effect should be considered.

In order to further reveal the reasons for the improvement of tensile properties of TMX-1.0 alloy in this study, summary of average grain size (d_{avg}), basal texture intensity and tensile properties in different Mg alloy systems are shown in **Table 1**. As shown in **Table 1**, TMX-1.0 alloy exhibits larger average grain size and higher texture intensity than most of other Mg-based alloys. It is therefore deduced that texture strengthening is the main reason for the improved properties of the studied alloy although grain boundary strengthening makes great contribution to TYS in this study.

CONCLUSIONS

A novel dilute TMX-1.0 alloy is developed and successful extruded with extrusion ration of 36. The extruded alloy exhibits fully recrystallized microstructure and ED-tilted basal texture. The average grain size and the texture intensity are 12.25 ± 0.15 μm and 9.23, respectively. In addition, some Mg2Sn and Mg2Ca nanoscale and/or sub-microscale precipitates are detected in certain micro-domains, with the morphology showing Mg_2Sn phase bordering Mg_2Ca. Moreover, the Meyer exponents n of the extruded dilute alloy is calculated to be 1.83 ± 0.063, indicating that an ISE behavior is observed in the present alloy system. The excellent combination of strength and ductility of the present alloy system are mainly ascribed to the relatively strong ED-tilted basal texture, and fine-grained structure as well as reasonable work-hardening exponent.

DATA AVAILABILITY STATEMENT

All datasets generated for this study are included in the article/supplementary material.

AUTHOR CONTRIBUTIONS

WC and CG: conceptualization. MH: methodology. XN and HW: software. LW: formal analysis. CG and MH: writing-original draft preparation. WC: writing-review and editing. MZ and JL: revised the manuscript.

FUNDING

This study was jointly supported by the National Natural Science Foundation of China (Grant Nos.:51704209, 51701060), Natural Science Foundation of Shanxi (201801D121088), a Research Project Supported by Shanxi Scholarship Council of China (Grant No.: 2014-023), and the Scientific and Technological Innovation Programs of Higher Education Institutions in Shanxi (Grant No.: 2014017) and the Shanxi Province Science Foundation for Youths (Grant No.: 2016021063).

REFERENCES

Bae, S. W., Kim, S. H., Lee, J. U., Jo, W. K., and Hong, W. H. (2018). Improvement of mechanical properties and reduction of yield asymmetry of extruded Mg-Al-Zn alloy through Sn addition. *J. Alloy. Comp.* 766, 748–758. doi: 10.1016/j.jallcom.2018.07.028

Chai, Y., Jiang, B., Song, J., Liu, B., Huang, G., Zhang, D., et al. (2019a). Effects of Zn and Ca addition on microstructure and mechanical properties

of as-extruded Mg-1.0Sn alloy sheet. *Mater. Sci. Eng. A* 746, 82–93. doi: 10.1016/j.msea.2019.01.028

Chai, Y., Jiang, B., Song, J., Wang, Q., Gao, H., Liu, B., et al. (2019b). Improvement of mechanical properties and reduction of yield asymmetry of extruded Mg-Sn-Zn alloy through Ca addition. *J. Alloy. Comp*. 782, 1076–1086. doi: 10.1016/j.jallcom.2018.12.109

Chen, C., Chen, J., Yan, H., Su, B., Song, M., and Zhu, S. (2016). Dynamic precipitation, microstructure and mechanical properties of Mg-5Zn-1Mn alloy sheets prepared by high strain-rate rolling. *Mater. Des.* 100, 58–66. doi: 10.1016/j.matdes.2016.03.129

Cheng, W., Bai, Y., Wang, L., Wang, H., Bian, L., and Yu, H. (2017a). Strengthening effect of extruded Mg-8Sn-2Zn-2Al alloy: influence of micro and nano-Size Mg_2Sn Precipitates. *Materials* 10:822. doi: 10.3390/ma10070822

Cheng, W., Tian, L., Ma, S., Bai, Y., and Wang, H. (2017b). Influence of equal channel angular pressing passes on the microstructures and tensile properties of Mg-8Sn-6Zn-2Al Alloy. *Materials* 10:708. doi: 10.3390/ma10070708

Cheng, W., Tian, L., Wang, H., Bian, L., and Yu, H. (2017c). Improved tensile properties of an equal channel angular pressed (ECAPed) Mg-8Sn-6Zn-2Al alloy by prior aging treatment. *Mater. Sci. Eng. A* 687, 148–154. doi: 10.1016/j.msea.2017.01.054

Cheng, W., Zhang, Y., Ma, S., Arthanari, S., Cui, Z., Wang, H. X., et al. (2018). Tensile properties and corrosion behavior of extruded low-alloyed Mg-1Sn-1Al-1Zn Alloy: the influence of microstructural characteristics. *Materials* 11:1157. doi: 10.3390/ma11071157

Cheng, W. L., Park, S. S., You, B. S., and Koo, B. H. (2010). Microstructure and mechanical properties of binary Mg–Sn alloys subjected to indirect extrusion. *Mater. Sci. Eng. A* 527, 4650–4653. doi: 10.1016/j.msea.2010.03.031

Cheng, W. L., Tian, Q. W., Yu, H., Zhang, H., and You, B. S. (2014). Strengthening mechanisms of indirect-extruded Mg–Sn based alloys at room temperature. *J. Magn. Alloys* 2, 299–304. doi: 10.1016/j.jma.2014.11.003

Fang, C., Wen, Z., Liu, X., Hao, H., Chen, G., and Zhang, X. (2017). Microstructures and mechanical properties of Mg 2 Sn-nanophase reinforced Mg–Mg 2 Sn composite. *Mater. Sci. Eng. A* 684, 229–232. doi: 10.1016/j.msea.2016.12.001

Hofstetter, J., Rüedi, S., Baumgartner, I., Kilian, H., Mingler, B., Povoden-Karadeniz, E., et al. (2015). Processing and microstructure–property relations of high-strength low-alloy (HSLA) Mg–Zn–Ca alloys. *Acta Mater*. 98, 423–432. doi: 10.1016/j.actamat.2015.07.021

Hu, K., Li, C., Xu, G., Ruizhen, G., Le, Q., and Liao, Q. (2019). Effect of extrusion temperature on the microstructure and mechanical properties of low Zn containing wrought Mg alloy micro-alloying with Mn and La-rich misch metal. *Mater. Sci. Eng. A* 742, 692–703. doi: 10.1016/j.msea.2018.10.068

Kim, S. H., and Park, S. H. (2016). Influence of Ce addition and homogenization temperature on microstructural evolution and mechanical properties of extruded Mg-Sn-Al-Zn alloy. *Mater. Sci. Eng. A* 676, 232–240. doi: 10.1016/j.msea.2016.08.093

Kim, S. H., You, B. S., and Park, S. H. (2017). Effect of billet diameter on hot extrusion behavior of Mg–Al–Zn alloys and its influence on microstructure and mechanical properties. *J. Alloy. Comp*. 690, 417–423. doi: 10.1016/j.jallcom.2016.08.144

Liao, H., Kim, J., Liu, T., Tang, A., She, J., Peng, P., et al. (2019). Effects of Mn addition on the microstructures, mechanical properties and work-hardening of Mg-1Sn alloy. *Mater. Sci. Eng. A* 754, 778–785. doi: 10.1016/j.msea.2019.02.021

Lu, X., Zhao, G., Zhou, J., Zhang, C., Chen, L., and Tang, S. (2018a). Microstructure and mechanical properties of Mg-3.0Zn-1.0Sn-0.3Mn-0.3Ca alloy extruded at different temperatures. J. *Alloy. Comp*. 732, 257–269. doi: 10.1016/j.jallcom.2017.10.210

Lu, X., Zhao, G., Zhou, J., Zhang, C., and Sun, L. (2018b). Effect of extrusion speeds on the microstructure, texture and mechanical properties of high-speed extrudable Mg Zn Sn Mn Ca alloy. *Vacuum* 157, 180–191. doi: 10.1016/j.vacuum.2018.08.041

Manika, I., and Maniks, J. (2006). Size effects in micro- and nanoscale indentation. *Acta Mater*. 54, 2049–2056. doi: 10.1016/j.actamat.2005.12.031

Nakata, T., Mezaki, T., Ajima, R., Xu, C., K., Oh-ishi, Shimizu, K., et al. (2015). High-speed extrusion of heat-treatable Mg–Al–Ca–Mn dilute alloy. *Scr. Mater.* 101, 28–31. doi: 10.1016/j.scriptamat.2015.01.010

Pan, H., Qin, G., Huang, Y., Ren, Y., Sha, X., Han, X., et al. (2018). Development of low-alloyed and rare-earth-free magnesium alloys having ultra-high strength. *Acta Mater*. 149, 350–363. doi: 10.1016/j.actamat.2018.03.002

Park, S. H., Jung, J. G., Yoon, J., and You, B. S. (2015). Influence of Sn addition on the microstructure and mechanical properties of extruded Mg−8Al−2Zn alloy. *Mater. Sci. Eng. A* 626, 128–135. doi: 10.1016/j.msea.2014.12.039

Park, S. H., Kim, S. H., Kim, H. S., Yoon, J., and You, B. S. (2016). High-speed indirect extrusion of Mg–Sn–Al–Zn alloy and its influence on microstructure and mechanical properties. *J. Alloy. Comp*. 667, 170–177. doi: 10.1016/j.jallcom.2016.01.163

Qi, F., Zhang, D., Zhang, X., and Xu, X. (2014). Effects of Mn addition and X-phase on the microstructure and mechanical properties of high-strength Mg–Zn–Y–Mn alloys. *Mater. Sci. Eng. A* 593, 70–78. doi: 10.1016/j.msea.2013.11.043

Robson, J. D., Henry, D. T., and Davis, B. (2009). Particle effects on recrystallization in magnesium–manganese alloys: particle-stimulated nucleation. *Acta Mater*. 57, 2739–2747. doi: 10.1016/j.actamat.2009.02.032

Sasaki, T. T., Yamamoto, K., Honma, T., Kamado, S., and Hono, K. (2008). A high-strength Mg–Sn–Zn–Al alloy extruded at low temperature. *Scr. Mater*. 59, 1111–1114. doi: 10.1016/j.scriptamat.2008.07.042

She, J., Pan, F., Zhang, J., Tang, A., Luo, S., Yu, Z., et al. (2016). Microstructure and mechanical properties of Mg–Al–Sn extruded alloys. *J. Alloy. Comp*. 657, 893–905. doi: 10.1016/j.jallcom.2015.10.146

Stanford, N., and Barnett, M. R. (2008). The origin of "rare earth" texture development in extruded Mg-based alloys and its effect on tensile ductility. *Mater. Sci. Eng. A* 496, 399–408. doi: 10.1016/j.msea.2008.05.045

Tang, W. N., Park, S. S., and You, B. S. (2011). Effect of the Zn content on the microstructure and mechanical properties of indirect-extruded Mg−5Sn–xZn alloys. *Mater. Des.* 32, 3537–3543. doi: 10.1016/j.matdes.2011.02.012

Tong, L. B., Zheng, M. Y., Xu, S. W., Kamado, S., Du, Y. Z., Hu, X. S., et al. (2011). Effect of Mn addition on microstructure, texture and mechanical properties of Mg–Zn–Ca alloy. *Mater. Sci. Eng. A* 528, 3741–3747. doi: 10.1016/j.msea.2011.01.037

Valdez, S., Suarez, M., Fregoso, O. A., and Juárez-Islas, J. A. (2012). Microhardness, microstructure and electrochemical efficiency of an Al (Zn/xMg) alloy after thermal treatment. *J. Mater. Sci. Technol*. 28, 255–260. doi: 10.1016/S1005-0302(12)60050-4

Wang, L., Mostaed, E., Cao, X., Huang, G., Fabrizi, A., Bonollo, F., et al. (2016). Effects of texture and grain size on mechanical properties of AZ80 magnesium alloys at lower temperatures. *Mater. Des.* 89, 1–8. doi: 10.1016/j.matdes.2015.09.153

Wang, Q., Shen, Y., Jiang, B., Tang, A., Song, J., Jiang, Z., et al. (2018). A micro-alloyed Mg-Sn-Y alloy with high ductility at room temperature. *Mater. Sci. Eng. A* 735, 131–144. doi: 10.1016/j.msea.2018.08.035

Wei, J., Chen, J., Yan, H., Su, B., and Pan, X. (2013). Effects of minor Ca addition on microstructure and mechanical properties of the Mg−4.5Zn−4.5Sn−2Al-based alloy system. *J. Alloy. Comp*. 548, 52–59. doi: 10.1016/j.jallcom.2012.08.102

Xiao, L., Yang, G., Chen, J., Luo, S., Li, J., and Jie, W. (2019). Microstructure, texture evolution and tensile properties of extruded Mg-4.58Zn-2.6Gd-0.16Zr alloy. *Mater. Sci. Eng. A* 744, 277–289. doi: 10.1016/j.msea.2018.11.142

Xu, D. K., and Han, E. H. (2012). Effects of icosahedral phase formation on the microstructure and mechanical improvement of Mg alloys: a review. *Prog. Nat. Sci-Mater*. 22, 364–385. doi: 10.1016/j.pnsc.2012.09.005

Yang, T. (2000). Study of the indentation size effect influencing microhardness measurement. *Chin. J. Rare Metals* 21. doi: 10.1007/s10019-003-0234-6

Yu, Z., Xu, C., Meng, J., Liu, K., Fu, J., and Kamado, S. (2019). Effects of extrusion ratio and temperature on the mechanical properties and microstructure of as-extruded Mg-Gd-Y-(Nd/Zn)-Zr alloys. *Mater. Sci. Eng. A* 762:138080. doi: 10.1016/j.msea.2019.138080

Zhang, B., Wang, Y., Geng, L., and Lu, C. (2012). Effects of calcium on texture and mechanical properties of hot-extruded Mg–Zn–Ca alloys. *Mater. Sci. Eng. A* 539, 56–60. doi: 10.1016/j.msea.2012.01.030

Zhao, C., Chen, X., Pan, F., Gao, S., Zhao, D., and Liu, X. (2018). Effect of Sn content on strain hardening behavior of as-extruded Mg-Sn alloys. *Mater. Sci. Eng. A* 713, 244–252. doi: 10.1016/j.msea.2017.12.074

Conflict of Interest: The authors declare that the research was conducted in the absence of any commercial or financial relationships that could be construed as a potential conflict of interest.